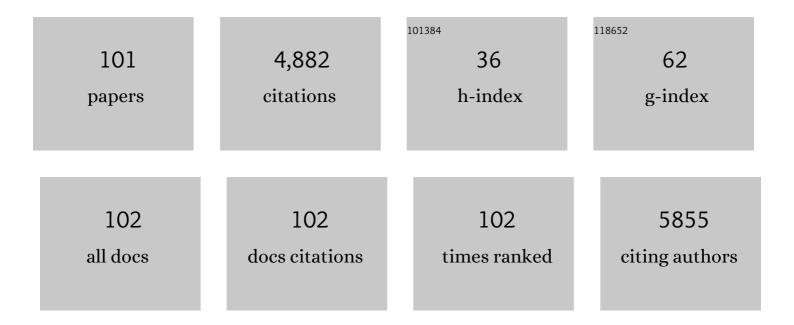
List of Publications by Year in descending order

Source: https://exaly.com/author-pdf/9478875/publications.pdf Version: 2024-02-01



ILANDING RIN

#	Article	IF	CITATIONS
1	Circular RNA Cdyl promotes abdominal aortic aneurysm formation by inducing M1 macrophage polarization and M1-type inflammation. Molecular Therapy, 2022, 30, 915-931.	3.7	46
2	CircRNA Chordc1 protects mice from abdominal aortic aneurysm by contributing to the phenotype and growth of vascular smooth muscle cells. Molecular Therapy - Nucleic Acids, 2022, 27, 81-98.	2.3	13
3	Evolution of tumor microenvironment in colorectal liver metastases under treatment stress. Cancer Communications, 2022, , .	3.7	0
4	CX3CL1 Worsens Cardiorenal Dysfunction and Serves as a Therapeutic Target of Canagliflozin for Cardiorenal Syndrome. Frontiers in Pharmacology, 2022, 13, 848310.	1.6	4
5	Pancreatic Adverse Events Associated With Immune Checkpoint Inhibitors: A Large-Scale Pharmacovigilance Analysis. Frontiers in Pharmacology, 2022, 13, 817662.	1.6	8
6	Optimal dose of physical exercise for preventing cardiac and renal dysfunction, data from National Health and Nutrition Examination Surveys survey. European Journal of Preventive Cardiology, 2022, 29, 1703-1706.	0.8	1
7	CircRNA Samd4 induces cardiac repair after myocardial infarction by blocking mitochondria-derived ROS output. Molecular Therapy, 2022, 30, 3477-3498.	3.7	34
8	Hydrogen sulfideâ€loaded microbubbles combined with ultrasound mediate thrombolysis and simultaneously mitigate ischemiaâ€reperfusion injury in a rat hindlimb model. Journal of Thrombosis and Haemostasis, 2021, 19, 738-752.	1.9	9
9	RNA interactions in right ventricular dysfunction induced type II cardiorenal syndrome. Aging, 2021, 13, 4215-4241.	1.4	9
10	Comprehensive analyses reveal TKI-induced remodeling of the tumor immune microenvironment in EGFR/ALK-positive non-small-cell lung cancer. Oncolmmunology, 2021, 10, 1951019.	2.1	33
11	Inhibition of SENP2-mediated Akt deSUMOylation promotes cardiac regeneration via activating Akt pathway. Clinical Science, 2021, 135, 811-828.	1.8	15
12	Long noncoding RNA (IncRNA) <i>EIF3J-DT</i> induces chemoresistance of gastric cancer via autophagy activation. Autophagy, 2021, 17, 4083-4101.	4.3	107
13	Immunosuppressive Microenvironment Revealed by Immune Cell Landscape in Pre-metastatic Liver of Colorectal Cancer. Frontiers in Oncology, 2021, 11, 620688.	1.3	9
14	Characterizing a long-term chronic heart failure model by transcriptomic alterations and monitoring of cardiac remodeling. Aging, 2021, 13, 13585-13614.	1.4	2
15	Antihypertrophic Memory After Regression of Exercise-Induced Physiological Myocardial Hypertrophy Is Mediated by the Long Noncoding RNA Mhrt779. Circulation, 2021, 143, 2277-2292.	1.6	45
16	IOBR: Multi-Omics Immuno-Oncology Biological Research to Decode Tumor Microenvironment and Signatures. Frontiers in Immunology, 2021, 12, 687975.	2.2	361
17	Growth differentiation factor 11 attenuates cardiac ischemia reperfusion injury via enhancing mitochondrial biogenesis and telomerase activity. Cell Death and Disease, 2021, 12, 665.	2.7	9
18	CRIP1 cooperates with BRCA2 to drive the nuclear enrichment of RAD51 and to facilitate homologous repair upon DNA damage induced by chemotherapy. Oncogene, 2021, 40, 5342-5355.	2.6	19

#	Article	IF	CITATIONS
19	Tumor microenvironment evaluation promotes precise checkpoint immunotherapy of advanced gastric cancer. , 2021, 9, e002467.		97
20	Single-cell analysis of a tumor-derived exosome signature correlates with prognosis and immunotherapy response. Journal of Translational Medicine, 2021, 19, 381.	1.8	14
21	Excessive fibroblast growth factor 23 promotes renal fibrosis in mice with type 2 cardiorenal syndrome. Aging, 2021, 13, 2982-3009.	1.4	16
22	LncRNA Snhg1-driven self-reinforcing regulatory network promoted cardiac regeneration and repair after myocardial infarction. Theranostics, 2021, 11, 9397-9414.	4.6	21
23	A Modified Surgical Ventricular Reconstruction in Post-infarction Mice Persistently Alleviates Heart Failure and Improves Cardiac Regeneration. Frontiers in Cardiovascular Medicine, 2021, 8, 789493.	1.1	4
24	Lansoprazole alleviates pressure overload-induced cardiac hypertrophy and heart failure in mice by blocking the activation of β-catenin. Cardiovascular Research, 2020, 116, 101-113.	1.8	32
25	Overexpression of Na+-HCO3– cotransporter contributes to the exacerbation of cardiac remodeling in mice with myocardial infarction by increasing intracellular calcium overload. Biochimica Et Biophysica Acta - Molecular Basis of Disease, 2020, 1866, 165623.	1.8	6
26	METTL3 Induces AAA Development and Progression by Modulating N6-Methyladenosine-Dependent Primary miR34a Processing. Molecular Therapy - Nucleic Acids, 2020, 21, 394-411.	2.3	34
27	circRNA Hipk3 Induces Cardiac Regeneration after Myocardial Infarction in Mice by Binding to Notch1 and miR-133a. Molecular Therapy - Nucleic Acids, 2020, 21, 636-655.	2.3	91
28	Macrophage correlates with immunophenotype and predicts anti-PD-L1 response of urothelial cancer. Theranostics, 2020, 10, 7002-7014.	4.6	108
29	Therapeutic ultrasound combined with microbubbles improves atherosclerotic plaque stability by selectively destroying the intraplaque neovasculature. Theranostics, 2020, 10, 2522-2537.	4.6	11
30	ltaconate prevents abdominal aortic aneurysm formation through inhibiting inflammation via activation of Nrf2. EBioMedicine, 2020, 57, 102832.	2.7	72
31	A stromaâ€related IncRNA panel for predicting recurrence and adjuvant chemotherapy benefit in patients with earlyâ€stage colon cancer. Journal of Cellular and Molecular Medicine, 2020, 24, 3229-3241.	1.6	18
32	A novel assessing system for predicting the prognosis of gastric cancer. Epigenomics, 2019, 11, 1251-1266.	1.0	2
33	Magnetic Targeting Improves the Therapeutic Efficacy of Microbubble-Mediated Obstructive Thrombus Sonothrombolysis. Thrombosis and Haemostasis, 2019, 119, 1752-1766.	1.8	9
34	Long noncoding RNA GAS5 induces abdominal aortic aneurysm formation by promoting smooth muscle apoptosis. Theranostics, 2019, 9, 5558-5576.	4.6	60
35	Suppression of miRNA let-7i-5p promotes cardiomyocyte proliferation and repairs heart function post injury by targetting CCND2 and E2F2. Clinical Science, 2019, 133, 425-441.	1.8	37
36	The pseudogene PTENP1 regulates smooth muscle cells as a competing endogenous RNA. Clinical Science, 2019, 133, 1439-1455.	1.8	26

#	Article	IF	CITATIONS
37	Relative Effect of Current Intensive Lipid-Lowering Drugs on Cardiovascular Outcomes in Secondary Prevention ― A Meta-Analysis of 12 Randomized Trials ―. Circulation Journal, 2019, 83, 1356-1367.	0.7	6
38	Gastric cancer cells escape metabolic stress via the DLC3/MACC1 axis. Theranostics, 2019, 9, 2100-2114.	4.6	11
39	LncRNA H19 promotes vascular inflammation and abdominal aortic aneurysm formation by functioning as a competing endogenous RNA. Journal of Molecular and Cellular Cardiology, 2019, 131, 66-81.	0.9	65
40	Response to: Cardiovascular events with blood pressure lowering in patients with diabetes and systolic blood pressure below 140 mm Hg. Journal of Clinical Hypertension, 2019, 21, 690-691.	1.0	0
41	miR-577 Regulates TGF-β Induced Cancer Progression through a SDPR-Modulated Positive-Feedback Loop with ERK-NF-βB in Gastric Cancer. Molecular Therapy, 2019, 27, 1166-1182.	3.7	35
42	Tumor Microenvironment Characterization in Gastric Cancer Identifies Prognostic and Immunotherapeutically Relevant Gene Signatures. Cancer Immunology Research, 2019, 7, 737-750.	1.6	691
43	A robust panel based on tumour microenvironment genes for prognostic prediction and tailoring therapies in stage l–III colon cancer. EBioMedicine, 2019, 42, 420-430.	2.7	46
44	Loss of Super-Enhancer-Regulated circRNA Nfix Induces Cardiac Regeneration After Myocardial Infarction in Adult Mice. Circulation, 2019, 139, 2857-2876.	1.6	284
45	ATXN2L upregulated by epidermal growth factor promotes gastric cancer cell invasiveness and oxaliplatin resistance. Cell Death and Disease, 2019, 10, 173.	2.7	47
46	Inhibition of AZIN2-sv induces neovascularization and improves prognosis after myocardial infarction by blocking ubiquitin-dependent talin1 degradation and activating the Akt pathway. EBioMedicine, 2019, 39, 69-82.	2.7	31
47	Long Non-coding RNA ECRAR Triggers Post-natal Myocardial Regeneration by Activating ERK1/2 Signaling. Molecular Therapy, 2019, 27, 29-45.	3.7	59
48	Immune cell infiltration as a biomarker for the diagnosis and prognosis of stage l–III colon cancer. Cancer Immunology, Immunotherapy, 2019, 68, 433-442.	2.0	209
49	SM22α (Smooth Muscle 22α) Prevents Aortic Aneurysm Formation by Inhibiting Smooth Muscle Cell Phenotypic Switching Through Suppressing Reactive Oxygen Species/NF-κB (Nuclear Factor-κB). Arteriosclerosis, Thrombosis, and Vascular Biology, 2019, 39, e10-e25.	1.1	64
50	Cardiovascular outcomes in patients with diabetes when initiating blood pressure lowering at baseline SBP between 130 and 140Âmm Hg: A metaâ€analysis. Journal of Clinical Hypertension, 2019, 21, 220-229.	1.0	4
51	Sirt1-inducible deacetylation of p21 promotes cardiomyocyte proliferation. Aging, 2019, 11, 12546-12567.	1.4	23
52	LncRNA Expression Profile of Human Thoracic Aortic Dissection by High-Throughput Sequencing. Cellular Physiology and Biochemistry, 2018, 46, 1027-1041.	1.1	27
53	Inhibition of <scp>SLC1A</scp> 5 sensitizes colorectal cancer to cetuximab. International Journal of Cancer, 2018, 142, 2578-2588.	2.3	38
54	Assessment of Thrombotic Risk in Atrial Fibrillation with Ultrasound Molecular Imaging of P-Selectin. Thrombosis and Haemostasis, 2018, 118, 388-400.	1.8	10

#	Article	IF	CITATIONS
55	Loss of AZIN2 splice variant facilitates endogenous cardiac regeneration. Cardiovascular Research, 2018, 114, 1642-1655.	1.8	65
56	Efficacy and safety of a 260-cm Amplatz Super Stiff guidewire during transradial percutaneous coronary intervention. Medicine (United States), 2018, 97, e12568.	0.4	2
57	Olmesartan attenuates pressure-overload- or post-infarction-induced cardiac remodeling in mice. Oncotarget, 2018, 9, 24601-24618.	0.8	1
58	Diagnostic Ultrasound and Microbubbles Treatment Improves Outcomes of Coronary No-Reflow in Canine Models by Sonothrombolysis. Critical Care Medicine, 2018, 46, e912-e920.	0.4	11
59	The effects of ultrasound exposure on P-glycoprotein-mediated multidrug resistance in vitro and in vivo. Journal of Experimental and Clinical Cancer Research, 2018, 37, 232.	3.5	18
60	Folate-conjugated nanobubbles selectively target and kill cancer cells via ultrasound-triggered intracellular explosion. Biomaterials, 2018, 181, 293-306.	5.7	50
61	Loss of long non-coding RNA CRRL promotes cardiomyocyte regeneration and improves cardiac repair by functioning as a competing endogenous RNA. Journal of Molecular and Cellular Cardiology, 2018, 122, 152-164.	0.9	50
62	IGF1/IGF1R/STAT3 signaling-inducible IFITM2 promotes gastric cancer growth and metastasis. Cancer Letters, 2017, 393, 76-85.	3.2	81
63	Long non-coding RNA MALAT1 promotes gastric cancer tumorigenicity and metastasis by regulating vasculogenic mimicry and angiogenesis. Cancer Letters, 2017, 395, 31-44.	3.2	176
64	MACC1 decreases the chemosensitivity of gastric cancer cells to oxaliplatin by regulating FASN expression. Oncology Reports, 2017, 37, 2583-2592.	1.2	29
65	Impact of remote ischaemic preconditioning on major clinical outcomes in patients undergoing cardiovascular surgery: A meta-analysis with trial sequential analysis of 32 randomised controlled trials. International Journal of Cardiology, 2017, 227, 882-891.	0.8	7
66	Bapx1 mediates transforming growth factor-β- induced epithelial-mesenchymal transition and promotes a malignancy phenotype of gastric cancer cells. Biochemical and Biophysical Research Communications, 2017, 486, 285-292.	1.0	9
67	TOP1MT deficiency promotes GC invasion and migration via the enhancements of LDHA expression and aerobic glycolysis. Endocrine-Related Cancer, 2017, 24, 565-578.	1.6	21
68	Contrast-Enhanced Ultrasound for Assessing Renal Perfusion Impairment and Predicting Acute Kidney Injury to Chronic Kidney Disease Progression. Antioxidants and Redox Signaling, 2017, 27, 1397-1411.	2.5	40
69	Comparison of Magnetic Microbubbles and Dual-modified Microbubbles Targeted to P-selectin for Imaging of Acute Endothelial Inflammation in the Abdominal Aorta. Molecular Imaging and Biology, 2017, 19, 183-193.	1.3	11
70	Ablation of periostin inhibits post-infarction myocardial regeneration in neonatal mice mediated by the phosphatidylinositol 3 kinase/glycogen synthase kinase 3î²/cyclin D1 signalling pathway. Cardiovascular Research, 2017, 113, 620-632.	1.8	84
71	Circular RNA expression profile and potential function of hsa_circRNA_101238 in human thoracic aortic dissection. Oncotarget, 2017, 8, 81825-81837.	0.8	48
72	FGF23 promotes myocardial fibrosis in mice through activation of β-catenin. Oncotarget, 2016, 7, 64649-64664.	0.8	100

#	Article	IF	CITATIONS
73	Clinical significance of accurate identification of lymph node status in distant metastatic gastric cancer. Oncotarget, 2016, 7, 1029-1041.	0.8	18
74	Overexpression of TRIB3 promotes angiogenesis in human gastric cancer. Oncology Reports, 2016, 36, 2339-2348.	1.2	23
75	Intensity of Left Atrial Spontaneous Echo Contrast as a Correlate for Stroke Risk Stratification in Patients with Nonvalvular Atrial Fibrillation. Scientific Reports, 2016, 6, 27650.	1.6	22
76	Loss of CEACAM1, a Tumor-Associated Factor, Attenuates Post-infarction Cardiac Remodeling by Inhibiting Apoptosis. Scientific Reports, 2016, 6, 21972.	1.6	21
77	Microbubble-Mediated Sonothrombolysis Improves Outcome After Thrombotic Microembolism-Induced Acute Ischemic Stroke. Stroke, 2016, 47, 1344-1353.	1.0	44
78	Voltageâ€gated sodium channel Na _v 1.7 promotes gastric cancer progression through MACC1â€mediated upregulation of NHE1. International Journal of Cancer, 2016, 139, 2553-2569.	2.3	64
79	Delivery of Hydrogen Sulfide by Ultrasound Targeted Microbubble Destruction Attenuates Myocardial Ischemia-reperfusion Injury. Scientific Reports, 2016, 6, 30643.	1.6	26
80	Elevated Orai1 and STIM1 expressions upregulate MACC1 expression to promote tumor cell proliferation, metabolism, migration, and invasion in human gastric cancer. Cancer Letters, 2016, 381, 31-40.	3.2	80
81	Ultrasound-targeted microbubble destruction enhances delayed BMC delivery and attenuates post-infarction cardiac remodelling by inducing engraftment signals. Clinical Science, 2016, 130, 2105-2120.	1.8	11
82	Acute hyperglycemia suppresses left ventricular diastolic function and inhibits autophagic flux in mice under prohypertrophic stimulation. Cardiovascular Diabetology, 2016, 15, 136.	2.7	26
83	Genome-wide analysis of alternative splicing during human heart development. Scientific Reports, 2016, 6, 35520.	1.6	29
84	Meta-analysis of two different surgical treatments of ischaemic mitral regurgitation with the same outcome: mitral valve repair vs mitral valve replacement. Acta Cardiologica, 2016, 71, 573-580.	0.3	1
85	MACC-1 Promotes Endothelium-Dependent Angiogenesis in Gastric Cancer by Activating TWIST1/VEGF-A Signal Pathway. PLoS ONE, 2016, 11, e0157137.	1.1	18
86	HMCB1-RAGE Axis Makes No Contribution to Cardiac Remodeling Induced by Pressure-Overload. PLoS ONE, 2016, 11, e0158514.	1.1	13
87	Selective depletion of tumor neovasculature by microbubble destruction with appropriate ultrasound pressure. International Journal of Cancer, 2015, 137, 2478-2491.	2.3	48
88	Overexpression of ankyrin repeat domain 1 enhances cardiomyocyte apoptosis by promoting p53 activation and mitochondrial dysfunction in rodents. Clinical Science, 2015, 128, 665-678.	1.8	33
89	High molecular weight chitosan derivative polymeric micelles encapsulating superparamagnetic iron oxide for tumor-targeted magnetic resonance imaging. International Journal of Nanomedicine, 2015, 10, 1155.	3.3	30
90	Detection of High-Risk Atherosclerotic Plaques with Ultrasound Molecular Imaging of Glycoprotein IIb/IIIa Receptor on Activated Platelets. Theranostics, 2015, 5, 418-430.	4.6	34

#	Article	IF	CITATIONS
91	Pharmacological modulation of autophagy to protect cardiomyocytes according to the time windows of ischaemia/reperfusion. British Journal of Pharmacology, 2015, 172, 3072-3085.	2.7	43
92	Effects of mineralocorticoid receptor antagonists in patients with preserved ejection fraction: a meta-analysis of randomized clinical trials. BMC Medicine, 2015, 13, 10.	2.3	27
93	Myocardial Hypertrophic Preconditioning Attenuates Cardiomyocyte Hypertrophy and Slows Progression to Heart Failure Through Upregulation of S100A8/A9. Circulation, 2015, 131, 1506-1517.	1.6	66
94	Flotillin-2 promotes nasopharyngeal carcinoma metastasis and is necessary for the epithelial-mesenchymal transition induced by transforming growth factor-l². Oncotarget, 2015, 6, 9781-9793.	0.8	44
95	MiR-338-3p inhibits epithelial-mesenchymal transition in gastric cancer cells by targeting ZEB2 and MACC1/Met/Akt signaling. Oncotarget, 2015, 6, 15222-15234.	0.8	98
96	Inhibition of microRNA-497 ameliorates anoxia/reoxygenation injury in cardiomyocytes by suppressing cell apoptosis and enhancing autophagy. Oncotarget, 2015, 6, 18829-18844.	0.8	64
97	Disruption of histamine H2 receptor slows heart failure progression through reducing myocardial apoptosis and fibrosis. Clinical Science, 2014, 127, 435-448.	1.8	51
98	A micrometer-sized ultrasound contrast agent with nanometer-scale polygonal patterning surfaces. Journal of Medical Ultrasonics (2001), 2014, 41, 421-429.	0.6	1
99	Effects of Beta-Blockers on Heart Failure with Preserved Ejection Fraction: A Meta-Analysis. PLoS ONE, 2014, 9, e90555.	1.1	73
100	Impact of Etiology on the Outcomes in Heart Failure Patients Treated with Cardiac Resynchronization Therapy: A Meta-Analysis. PLoS ONE, 2014, 9, e94614.	1.1	23
101	Cytosolic CARP Promotes Angiotensin II- or Pressure Overload-Induced Cardiomyocyte Hypertrophy through Calcineurin Accumulation. PLoS ONE, 2014, 9, e104040.	1.1	16